NEWTONIAN GRAVITATIONAL N-BODY SPHERICAL SIMPLIFICATION ALGORITHM IN RIEMANNIAN DUAL SPACE-TIME

N. O. Schmidt
Department of Mathematics,
Boise State University,
1910 University Drive,
Boise, Idaho, 83725, USA
nathanschmidt@u.boisestate.edu

February 2013

Abstract

We propose a *preliminary* algorithm which is designed to reduce aspects of the n-body problem to a 2-body problem for holographic principle compliance. The objective is to share an alternative view-point on the n-body problem to try and generate a simple solution in the near future. The algorithm operates complex and triplex data structures to encode the chaotic dynamical system equipped with order parameter fields in both 3D and 4D versions of the Riemannian dual (fractional quantum Hall superfluidic) space-time topology. For the algorithm, we arbitrarily select one point-mass to be the origin and, from that reference frame, we subsequently engage a series of instructions to consolidate the residual $(n-1)$-bodies to a time-effective spherical surface. Through a step-by-step example, we demonstrate that the algorithm yields time-effective net-quantities that authorize us to define a time-effective potential, kinetic, and Lagrangian.

Keywords: Newtonian mechanics; Relativistic mechanics; Gravitation; Holographic principle; Holographic ring; Riemannian circle; Riemann surface; Space-time duality; Topology; Generalized coordinates; Complex numbers; Triplex numbers; Chaos; Spontaneous symmetry breaking; Order parameters.

1 Introduction

The n-body problem is the problem of predicting the motion of a group of celestial objects that gravitationally interact with each other [1, 2]. Solving this problem has been motivated by the need to understand the motion of, for example, planets, stars, and black holes. Its first complete mathematical formulation appeared in Isaac Newton's Principia [1, 2]. Since gravity is responsible for the motion of planets and stars, Newton had to express gravitational interactions in terms of differential equations [1, 2]. In the Principia [1, 2], Newton proved that a spherically-symmetric body can be modeled as a point-mass. Interestingly, quantized particles may also modeled as point-masses [3, 4, 5, 6], which seems to indicate that a solution to the n-body problem may be applied to a future unified theory of quantum gravity. To date, the 2-body problem has been completely solved, but only certain solutions exist for the 3-body problem [7].

Over a century ago, Poincaré's work on the *restricted* version of the 3-body problem formed the foundation of deterministic chaos theory [7]. Chaos theory studies the behavior of dynamical systems that are highly sensitive to initial conditions [8, 9]. In a chaotic dynamical system, miniscule differences in initial conditions yield widely diverging outcomes, thereby generally rendering long-term predictions impossible [8, 9]. Chaos is abundant in nature [9, 10, 11], and such complex systems are widely studied in computation, mathematics, science, and engineering. In addition to quantum and astro physics, examples of chaos are also observed in weather patterns [12], aquatic ecosystems [13], population biology [14], cancers and genetics [15, 16], viruses and pathogens [17], earthquakes [18, 19], volcanoes [20], and the global stock market [21]. Moreover, we note that fractals are the language of chaos theory [22], where fractals are clearly everywhere in nature [23] including, for example, the allometric scaling laws in biology [24, 25, 26, 27, 28]. The plethora of well-documented scientific evidence for naturally-recurring n-body problems fundamentally conveys the significance pertaining to this mode of research. Thus, it is imperative to investigate such phenomenon from diverse perspectives and attack these problems from multiple directions.

In this introductory paper, we propose the *Newtonian Gravitational n-Body Spherical Simplification Algorithm* (NGNBSSA), which aims to simplify the apparent complexity of the *unrestricted* version of the $(n > 2)$-body problem to that of a 2-body problem, for which the $n = 2$ solution *does exist*; the objective is to share an alternative view-point on the n-body problem to try and generate a solution in the near future. The NGNBSSA is a well-defined procedure of instructions that engages the complex and triplex data structure framework of [29] to encode 3D and 4D versions of the Riemannian dual (fractional quantum Hall superfluidic) space-time topology [30] equipped with order parameter fields.

In Section 2, we prepare for our systematic n-body attack by assembling the requisite data structures for characterizing the chaotic gravitational system state space. First, in Section 2.1, we devise the complex data structures for encoding 2D locations and 2D features in the Riemannian dual 3D space-time topology of [29, 30]. Subsequently, in Section 2.2, we contrive the triplex data structures for encoding 3D locations and 3D features in the Riemannian dual 4D space-time topology of [29].

In Section 3, we present the NGNBSSA via a step-by-step example of instructions and illustrations. Section 3.1 demonstrates how the NGNBSSA systematically operates in the Riemannian dual 3D space-time topology with the complex encoding framework [29, 30], while Section 3.2 explains how to adjust the NGNBSSA so it can also function in the Riemannian dual 4D space-time topology with the triplex encoding framework [29]. In both scenarios, we use the results to define a time-effective potential, kinetic, and Lagrangian that intertwine mechanics from Newton and Einstein.

The paper terminates with the conclusive discussion and future outlook of Section 4, followed by the brief concessions of Section 5.

2 Data structures

In this section, we prepare for the NGNBSSA by assembling the chaotic gravitational system state space for encoding locations and features in the Riemannian dual 3D *and* 4D space-time topologies [29, 30].

2.1 Complex structures in dual 3D space-time

To encode complex locations, we identify the Riemann surface X as the *2D Position-Point State Space* (2D-PPSS) [29, 30]. Thus, we let

$$P_X \subset X = \{\vec{x}_1, \vec{x}_2, ..., \vec{x}_n\} \tag{1}$$

be the ordered set of spherically-symmetric point-particles of cardinality $n = |P_X|$ with the corresponding *2D Riemannian-coordinates* [29, 30]

$$\begin{array}{rcl} 1: \;\; \vec{x}_1 & = & (\vec{x}_1) = (|\vec{x}_1|, \langle\vec{x}_1\rangle) = (\vec{x}_{1_{\mathbb{R}}}, \vec{x}_{1_{\mathbb{I}}}) \\ 2: \;\; \vec{x}_2 & = & (\vec{x}_2) = (|\vec{x}_2|, \langle\vec{x}_2\rangle) = (\vec{x}_{2_{\mathbb{R}}}, \vec{x}_{2_{\mathbb{I}}}) \\ & ... & \\ n: \;\; \vec{x}_n & = & (\vec{x}_n) = (|\vec{x}_n|, \langle\vec{x}_n\rangle) = (\vec{x}_{n_{\mathbb{R}}}, \vec{x}_{n_{\mathbb{I}}}). \end{array} \tag{2}$$

Each point-particle in P_X has a location that is a *2D Position-Point State* (2D-PPS) from [29, 30]. For P_X in eq. (1), we let

$$M_X = \{m_1, m_2, ..., m_n\} \tag{3}$$

be the corresponding ordered set of non-zero *2D Position-Point-Masses* (2D-PPM) of cardinality $n = |M_X|$. Moreover, each point-particle in P_X also has a velocity that is a *2D Velocity Field Order Parameter State* (2D-VFOPS) defined using the 2D-OPS notation of [29]. Hence, we let

$$V_X = \{\vec{v}_1, \vec{v}_2, ..., \vec{v}_n\} = \{\vec{\psi}_v(\vec{x}_1), \vec{\psi}_v(\vec{x}_2), ..., \vec{\psi}_v(\vec{x}_n)\} \tag{4}$$

be the ordered 2D-VFOPS set of cardinality $n = |V_X|$ with the corresponding definitions

$$\begin{array}{rcl} 1: \;\; \vec{v}_1 & \equiv & \vec{v}_{1_{\mathbb{R}}} + \vec{v}_{1_{\mathbb{I}}} \equiv (\vec{v}_1) \equiv \vec{\psi}_v(\vec{x}_1) \equiv (|\vec{v}_1|, \langle\vec{v}_1\rangle) \equiv (\vec{v}_{1_{\mathbb{R}}}, \vec{v}_{1_{\mathbb{I}}}) \\ 2: \;\; \vec{v}_2 & \equiv & \vec{v}_{2_{\mathbb{R}}} + \vec{v}_{2_{\mathbb{I}}} \equiv (\vec{v}_2) \equiv \vec{\psi}_v(\vec{x}_2) \equiv (|\vec{v}_2|, \langle\vec{v}_2\rangle) \equiv (\vec{v}_{2_{\mathbb{R}}}, \vec{v}_{2_{\mathbb{I}}}) \\ & ... & \\ n: \;\; \vec{v}_n & \equiv & \vec{v}_{n_{\mathbb{R}}} + \vec{v}_{n_{\mathbb{I}}} \equiv (\vec{v}_n) \equiv \vec{\psi}_v(\vec{x}_n) \equiv (|\vec{v}_n|, \langle\vec{v}_n\rangle) \equiv (\vec{v}_{n_{\mathbb{R}}}, \vec{v}_{n_{\mathbb{I}}}). \end{array} \tag{5}$$

Next, we apply Newton's law of universal gravitation to M_X for P_X across X, where the force between between any two 2D-PPM is directly proportional to their product and inversely proportional to the square of the distance between them [1, 2]. To encode the gravitational force between two such bodies in 3D space-time, say $m_i, m_j \in M_X$ for $i \neq j$ and $1 \leq i, j \leq n$, we adopt and adjust the 2D-OPS notation of eq. (23) in [29] and add a second 2D-PPS argument to define the *2D Newtonian Force Field Order Parameter State* (2D-NFFOPS)

$$\begin{aligned}\vec{F}_{ij} &\equiv \vec{F}_{ij_{\mathbb{R}}} + \vec{F}_{ij_{\mathbb{I}}} \equiv \left(\vec{F}_{ij}\right) \equiv \left(\vec{F}_{ij_{\mathbb{R}}}, \vec{F}_{ij_{\mathbb{I}}}\right) \equiv \left(|\vec{F}_{ij}|, \langle \vec{F}_{ij} \rangle\right) \\ &\equiv \vec{\psi}_F(\vec{x}_i, \vec{x}_j) \equiv \vec{\psi}_F(\vec{x}_i, \vec{x}_j)_{\mathbb{R}} + \vec{\psi}_F(\vec{x}_i, \vec{x}_j)_{\mathbb{I}} \equiv \left(\vec{\psi}_F(\vec{x}_i, \vec{x}_j)\right) \\ &\equiv \left(\vec{\psi}_F(\vec{x}_i, \vec{x}_j)_{\mathbb{R}}, \vec{\psi}_F(\vec{x}_i, \vec{x}_j)_{\mathbb{I}}\right) \equiv \left(|\vec{\psi}_F(\vec{x}_i, \vec{x}_j)|, \langle \vec{\psi}_F(\vec{x}_i, \vec{x}_j) \rangle\right)\end{aligned} \tag{6}$$

from the perspective of $\vec{x}_i$ to $\vec{x}_j$, which applies to all such pairs in P_X. Hence, the 2D-OPS component constraints and notations of eqs. (18–25) in [29] apply to the 2D-NFFOPS definition of eq. (6). Therefore, $\forall \vec{x}_i, \vec{x}_j \in P_X$ the gravitational 2D-NFFOPS-amplitude between $m_i, m_j \in M_X$ is

$$\begin{aligned}|\vec{F}_{ij}| &\equiv \sqrt{\vec{F}^2_{ij_{\mathbb{R}}} + \vec{F}^2_{ij_{\mathbb{I}}}} \equiv G\tfrac{m_i m_j}{d^2_{ij}} \\ &\equiv |\vec{\psi}_F(\vec{x}_i, \vec{x}_j)| \equiv \sqrt{\vec{\psi}^2_F(\vec{x}_i, \vec{x}_j)_{\mathbb{R}} + \vec{\psi}^2_F(\vec{x}_i, \vec{x}_j)_{\mathbb{I}}},\end{aligned} \tag{7}$$

where G is the gravitational constant and d_{ij} is defined as the Euclidean distance

$$d_{ij} = d(\vec{x}_i, \vec{x}_j) = \sqrt{(\vec{x}_{j_{\mathbb{R}}} - \vec{x}_{i_{\mathbb{R}}})^2 + (\vec{x}_{j_{\mathbb{I}}} - \vec{x}_{i_{\mathbb{I}}})^2} \tag{8}$$

between $\vec{x}_i$ and $\vec{x}_j$ using the 2D-PPS Cartesian-coordinate properties for the geometrical line segment $\overline{\vec{x}_i \vec{x}_j}$.

Now, we can simplify the notation of eqs. (6–8) even further if we let $\vec{x}_i = O$ be the origin-point of eq. (10) in [29] with the 2D-PPM re-labeling $m_O = m_i$. Thus, $\forall \vec{x}_j \in P_X$, eq. (6) is re-written as

$$\vec{F}_j \equiv \vec{\psi}_F(O, \vec{x}_j) \equiv \vec{F}_{j_{\mathbb{R}}} + \vec{F}_{j_{\mathbb{I}}} \equiv \left(\vec{F}_j\right) \equiv \left(\vec{F}_{j_{\mathbb{R}}}, \vec{F}_{j_{\mathbb{I}}}\right) \equiv \left(|\vec{F}_j|, \langle \vec{F}_j \rangle\right), \tag{9}$$

with respect to O, which clearly satisfies the 2D-OPS component constraints and notations of eqs. (18–25) in [29]. Therefore, eq. (7) is re-written as

$$|\vec{F}_j| \equiv |\vec{\psi}_F(O, \vec{x}_j)| \equiv \sqrt{\vec{F}^2_{j_{\mathbb{R}}} + \vec{F}^2_{j_{\mathbb{I}}}} \equiv G\frac{m_O m_j}{d^2_j}, \tag{10}$$

where d_j is defined as the Euclidean distance by re-writing eq. (8) as

$$d_j = d(O, \vec{x}_j) = \sqrt{(\vec{x}_{j_{\mathbb{R}}} - O_{\mathbb{R}})^2 + (\vec{x}_{j_{\mathbb{I}}} - O_{\mathbb{I}})^2} = |\vec{x}_j| \tag{11}$$

between O and $\vec{x}_j$, which is the 2D-PPS-amplitude that corresponds to the geometrical line segment $\overline{O\vec{x}_j}$.

At this point, we have both the $\vec{F}_j$ of eq. (9) and the $m_j \in M_X$ of eq. (3), so Newton's second law [1, 2] comes to mind. Thus, using the same notation of eq. (9), we define the *2D Newtonian Acceleration Field Order Parameter State* (2D-NAFOPS)

$$\vec{a}_j \equiv \vec{\psi}_a(O, \vec{x}_j) \equiv \vec{a}_{j_{\mathbb{R}}} + \vec{a}_{j_{\mathbb{I}}} \equiv (\vec{a}_j) \equiv (\vec{a}_{j_{\mathbb{R}}}, \vec{a}_{j_{\mathbb{I}}}) \equiv (|\vec{a}_j|, \langle \vec{a}_j \rangle)\,, \tag{12}$$

with respect to O, where the 2D-NAFOPS-amplitude is defined as

$$|\vec{a}_j| \equiv |\vec{\psi}_a(O, \vec{x}_j)| \equiv \sqrt{\vec{a}^2_{j_{\mathbb{R}}} + \vec{a}^2_{j_{\mathbb{I}}}} \equiv \frac{|\vec{F}_j|}{m_j}. \tag{13}$$

Hence, the 2D-NFFOPS-phase, 2D-NAFOPS-phase, and 2D-PPS-phase bestow the equivalence

$$\langle \vec{F}_j \rangle \equiv \langle \vec{a}_j \rangle \equiv \langle \vec{x}_j \rangle. \tag{14}$$

The next step is to define, relative to m_O with v_O, the *2D Relative Velocity Field Order Parameter State* (2D-RVFOPS) for some m_j with v_j as

$$\vec{\vartheta}_j \equiv \vec{\psi}_\vartheta(O, \vec{x}_j) \equiv \vec{\vartheta}_{j_{\mathbb{R}}} + \vec{\vartheta}_{j_{\mathbb{I}}} \equiv \left(\vec{\vartheta}_j\right) \equiv \left(\vec{\vartheta}_{j_{\mathbb{R}}}, \vec{\vartheta}_{j_{\mathbb{I}}}\right) \equiv \left(|\vec{\vartheta}_j|, \langle \vec{\vartheta}_j \rangle\right), \tag{15}$$

such that

$$\begin{aligned} \vec{\vartheta}_{j_{\mathbb{R}}} &\equiv \vec{v}_{j_{\mathbb{R}}} - \vec{v}_{O_{\mathbb{R}}} \\ \vec{\vartheta}_{j_{\mathbb{I}}} &\equiv \vec{v}_{j_{\mathbb{I}}} - \vec{v}_{O_{\mathbb{I}}}, \end{aligned} \tag{16}$$

where from eq. (22) in [29] we establish

$$\begin{aligned} |\vec{\vartheta}_j| &\equiv \sqrt{\vec{\vartheta}^2_{j_{\mathbb{R}}} + \vec{\vartheta}^2_{j_{\mathbb{I}}}} \\ \vec{\vartheta}_{j_{\mathbb{R}}} &\equiv |\vec{\vartheta}_j| \cos\langle \vec{\vartheta}_j \rangle \\ \vec{\vartheta}_{j_{\mathbb{I}}} &\equiv |\vec{\vartheta}_j| \sin\langle \vec{\vartheta}_j \rangle, \end{aligned} \tag{17}$$

which is clearly similar to the constraints of eqs. (9) and (12) that follow [29].

We note that the circular time-dimension $T \subset X$ in eq. (13) of [29] with amplitude-radius ϵ does apply to this scenario, but we must wait to establish T in Section 3.1 because the value of ϵ depends on the NGNBSSA's intermediate results. A 2D-PPS that exists in T is defined as a *time-effective 2D-PPS* (TE-2D-PPS); the 2D-PPM, 2D-NFFOPS, 2D-NAFOPS, 2D-VFOPS, and 2D-RVFOPS for a TE-2D-PPS are defined as the *time-effective 2D-PPM* (TE-2D-PPM), *time-effective 2D-NFFOPS* (TE-2D-NFFOPS), *time-effective 2D-NAFOPS* (TE-2D-NAFOPS), *time-effective 2D-VFOPS* (TE-2D-VFOPS), and *time-effective 2D-RVFOPS* (TE-2D-RVFOPS), respectively. Thus, at this point, we can encode the relevant chaotic dynamical system states in the Riemannian dual 3D space-time of [29, 30] for the upcoming NGNBSSA in Section 3.1.

2.2 Triplex structures in dual 4D space-time

Here, we project the complex structures of Section 2.1 to a higher dimensional structure with an additional degree of freedom.

First, we project the complex locations of eqs. (1–2) in accordance to [29]. Thus, to encode triplex locations, we identify the 3D real manifold Y as the *3D Position-Point State Space* (3D-PPSS), such that $X \subset Y$ [29]. Thus, we let

$$P_Y \subset Y = \{\vec{y}_1, \vec{y}_2, ..., \vec{y}_n\} \tag{18}$$

be the ordered set of spherically-symmetric point-particles of cardinality $n = |P_Y|$ with the corresponding *3D Riemannian-coordinates* [29]

$$\begin{array}{rcl} 1: \;\; \vec{y}_1 & = & (\vec{y}_1) = (|\vec{y}_1|, \langle\vec{y}_1\rangle, [\vec{y}_1]) = (\vec{y}_{1_\mathbb{R}}, \vec{y}_{1_\mathbb{I}}, \vec{y}_{1_Z}) \\ 2: \;\; \vec{y}_2 & = & (\vec{y}_2) = (|\vec{y}_2|, \langle\vec{y}_2\rangle, [\vec{y}_2]) = (\vec{y}_{2_\mathbb{R}}, \vec{y}_{2_\mathbb{I}}, \vec{y}_{2_Z}) \\ & ... & \\ n: \;\; \vec{y}_n & = & (\vec{y}_n) = (|\vec{y}_n|, \langle\vec{y}_n\rangle, [\vec{y}_n]) = (\vec{y}_{n_\mathbb{R}}, \vec{y}_{n_\mathbb{I}}, \vec{y}_{n_Z}). \end{array} \tag{19}$$

Each point-particle in P_Y has a location that is a *3D Position-Point State* (3D-PPS) from [29]. For P_Y in eq. (18), we let

$$M_Y = \{m_1, m_2, ..., m_n\} \tag{20}$$

be the corresponding ordered set of non-zero *3D Position-Point-Masses* (3D-PPM) of cardinality $n = |M_Y|$. Moreover, each point-particle in P_Y also has a velocity that is a *3D Velocity Field Order Parameter State* (3D-VFOPS) defined using the 3D-OPS notation of [29]. Hence, we let

$$V_Y = \{\vec{v}_1, \vec{v}_2, ..., \vec{v}_n\} = \{\vec{\psi}_v(\vec{y}_1), \vec{\psi}_v(\vec{y}_2), ..., \vec{\psi}_v(\vec{y}_n)\} \tag{21}$$

be the ordered 3D-VFOPSs set of cardinality $n = |V_Y|$ with the corresponding definitions

$$\begin{array}{rcl} 1: \;\; \vec{v}_1 & \equiv & \vec{v}_{1_\mathbb{R}} + \vec{v}_{1_\mathbb{I}} + \vec{v}_{1_Z} \equiv (\vec{v}_1) \equiv \vec{\psi}_v(\vec{y}_1) \equiv (|\vec{v}_1|, \langle\vec{v}_1\rangle, [\vec{v}_1]) \equiv (\vec{v}_{1_\mathbb{R}}, \vec{v}_{1_\mathbb{I}}, \vec{v}_{1_Z}) \\ 2: \;\; \vec{v}_2 & \equiv & \vec{v}_{2_\mathbb{R}} + \vec{v}_{2_\mathbb{I}} + \vec{v}_{2_Z} \equiv (\vec{v}_2) \equiv \vec{\psi}_v(\vec{y}_2) \equiv (|\vec{v}_2|, \langle\vec{v}_2\rangle, [\vec{v}_2]) \equiv (\vec{v}_{2_\mathbb{R}}, \vec{v}_{2_\mathbb{I}}, \vec{v}_{2_Z}) \\ & ... & \\ n: \;\; \vec{v}_n & \equiv & \vec{v}_{n_\mathbb{R}} + \vec{v}_{n_\mathbb{I}} + \vec{v}_{n_Z} \equiv (\vec{v}_n) \equiv \vec{\psi}_v(\vec{y}_n) \equiv (|\vec{v}_n|, \langle\vec{v}_n\rangle, [\vec{v}_n]) \equiv (\vec{v}_{n_\mathbb{R}}, \vec{v}_{n_\mathbb{I}}, \vec{v}_{n_Z}). \end{array} \tag{22}$$

Next, we apply Newton's law of universal gravitation [1, 2] to M_Y for P_Y across Y. To encode the gravitational force between two such 3D-PPMs in 3D space-time, say $m_i, m_j \in M_Y$ for $i \neq j$ and $1 \leq i, j \leq n$, we adopt and adjust the 3D-OPS notation of eq. (50) in [29] and add a second 3D-PPS argument to define the *3D Newtonian Force Field Order Parameter State* (3D-NFFOPS)

$$\begin{aligned} \vec{F}_{ij} & \equiv \vec{F}_{ij_\mathbb{R}} + \vec{F}_{ij_\mathbb{I}} + \vec{F}_{ij_Z} \equiv \left(\vec{F}_{ij}\right) \equiv \left(\vec{F}_{ij_\mathbb{R}}, \vec{F}_{ij_\mathbb{I}}, \vec{F}_{ij_Z}\right) \equiv \left(|\vec{F}_{ij}|, \langle\vec{F}_{ij}\rangle, [\vec{F}_{ij}]\right) \\ & \equiv \vec{\psi}_F(\vec{y}_i, \vec{y}_j) \equiv \vec{\psi}_F(\vec{y}_i, \vec{y}_j)_\mathbb{R} + \vec{\psi}_F(\vec{y}_i, \vec{y}_j)_\mathbb{I} + \vec{\psi}_F(\vec{y}_i, \vec{y}_j)_Z \equiv \left(\vec{\psi}_F(\vec{y}_i, \vec{y}_j)\right) \\ & \equiv \left(\vec{\psi}_F(\vec{y}_i, \vec{y}_j)_\mathbb{R}, \vec{\psi}_F(\vec{y}_i, \vec{y}_j)_\mathbb{I}, \vec{\psi}_F(\vec{y}_i, \vec{y}_j)_Z\right) \equiv \left(|\vec{\psi}_F(\vec{y}_i, \vec{y}_j)|, \langle\vec{\psi}_F(\vec{y}_i, \vec{y}_j)\rangle, [\vec{\psi}_F(\vec{y}_i, \vec{y}_j)]\right) \end{aligned} \tag{23}$$

from the perspective of $\vec{y}_i$ to $\vec{y}_j$, which applies to all such pairs in P_Y. Hence, the 3D-OPS component constraints and notations of eqs. (45–52) in [29] apply to the 3D-NFFOPS definition of eq. (23). Therefore, $\forall \vec{y}_i, \vec{y}_j \in P_Y$ the gravitational 3D-NFFOPS-amplitude between $m_i, m_j \in M_Y$ is

$$\begin{aligned} |\vec{F}_{ij}| &\equiv \sqrt{\vec{F}^2_{ij_{\mathbb{R}}} + \vec{F}^2_{ij_{\mathbb{I}}} + \vec{F}^2_{ij_Z}} \equiv G\tfrac{m_i m_j}{d^2_{ij}} \\ &\equiv |\vec{\psi}_F(\vec{y}_i, \vec{y}_j)| \equiv \sqrt{\vec{\psi}^2_F(\vec{y}_i, \vec{y}_j)_{\mathbb{R}} + \vec{\psi}^2_F(\vec{y}_i, \vec{y}_j)_{\mathbb{I}} + \vec{\psi}^2_F(\vec{y}_i, \vec{y}_j)_Z}, \end{aligned} \tag{24}$$

where d_{ij} is defined as the Euclidean distance

$$d_{ij} = d(\vec{y}_i, \vec{y}_j) = \sqrt{(\vec{y}_{j_{\mathbb{R}}} - \vec{y}_{i_{\mathbb{R}}})^2 + (\vec{y}_{j_{\mathbb{I}}} - \vec{y}_{i_{\mathbb{I}}})^2 + (\vec{y}_{j_Z} - \vec{y}_{i_Z})^2} \tag{25}$$

between $\vec{y}_i$ and $\vec{y}_j$ using the 3D-PPS Cartesian-coordinate properties for the geometrical line segment $\overline{\vec{y}_i\vec{y}_j}$.

Now, we can simplify the notation of eqs. (23–25) even further if we let $\vec{y}_i = O$ be the 3D version of the origin-point in [29] with the 3D-PPM re-labeling $m_O = m_i$. Thus, $\forall \vec{y}_j \in P_Y$, eq. (23) is re-written as

$$\vec{F}_j \equiv \vec{\psi}_F(O, \vec{y}_j) \equiv \vec{F}_{j_{\mathbb{R}}} + \vec{F}_{j_{\mathbb{I}}} + \vec{F}_{j_Z} \equiv \left(\vec{F}_j\right) \equiv \left(\vec{F}_{j_{\mathbb{R}}}, \vec{F}_{j_{\mathbb{I}}}, \vec{F}_{j_Z}\right) \equiv \left(|\vec{F}_j|, \langle\vec{F}_j\rangle, [\vec{F}_j]\right), \tag{26}$$

with respect to O, which clearly satisfies the 3D-OPS component constraints and notations of eqs. (45–52) in [29]. Therefore, eq. (24) is re-written as

$$|\vec{F}_j| \equiv |\vec{\psi}_F(O, \vec{y}_j)| \equiv \sqrt{\vec{F}^2_{j_{\mathbb{R}}} + \vec{F}^2_{j_{\mathbb{I}}} + \vec{F}^2_{j_Z}} \equiv G\frac{m_O m_j}{d^2_j}, \tag{27}$$

where d_j is defined as the Euclidean distance by re-writing eq. (25) as

$$d_j = d(O, \vec{y}_j) = \sqrt{(\vec{y}_{j_{\mathbb{R}}} - O_{\mathbb{R}})^2 + (\vec{y}_{j_{\mathbb{I}}} - O_{\mathbb{I}})^2 + (\vec{y}_{j_Z} - O_Z)^2} = |\vec{y}_j| \tag{28}$$

between O and $\vec{y}_j$, which is the 3D-PPS-amplitude that corresponds to the geometrical line segment $\overline{O\vec{y}_j}$.

At this point, we have both the $\vec{F}_j$ of eq. (26) and the $m_j \in M_Y$ of eq. (20), so again we recall Newton's second law [1, 2]. Thus, using the same notation of eq. (26), we define the *3D Newtonian Acceleration Field Order Parameter State* (3D-NAFOPS)

$$\vec{a}_j \equiv \vec{\psi}_a(O, \vec{x}_j) \equiv \vec{a}_{j_{\mathbb{R}}} + \vec{a}_{j_{\mathbb{I}}} + \vec{a}_{j_Z} \equiv (\vec{a}_j) \equiv (\vec{a}_{j_{\mathbb{R}}}, \vec{a}_{j_{\mathbb{I}}}, \vec{a}_{j_Z}) \equiv (|\vec{a}_j|, \langle\vec{a}_j\rangle, [\vec{a}_j]), \tag{29}$$

with respect to O, where the 3D-NAFOPS-amplitude is defined as

$$|\vec{a}_j| \equiv |\vec{\psi}_a(O, \vec{x}_j)| \equiv \sqrt{\vec{a}^2_{j_{\mathbb{R}}} + \vec{a}^2_{j_{\mathbb{I}}} + \vec{a}^2_{j_Z}} \equiv \frac{|\vec{F}_j|}{m_j}. \tag{30}$$

Hence, the 3D-NFFOPS-phase, 3D-NAFOPS-phase, and 3D-PPS-phase bestow the equivalence

$$\langle \vec{F}_j \rangle \equiv \langle \vec{a}_j \rangle \equiv \langle \vec{y}_j \rangle, \tag{31}$$

while the 3D-NFFOPS-inclination, 3D-NAFOPS-inclination, and 3D-PPS-inclination similarly yield

$$[\vec{F}_j] \equiv [\vec{a}_j] \equiv [\vec{y}_j]. \tag{32}$$

The next step is to define, relative to m_O with v_O, the *3D Relative Velocity Field Order Parameter State* (3D-RVFOPS) for some m_j with v_j as

$$\vec{\vartheta}_j \equiv \vec{\psi}_\vartheta(O, \vec{y}_j) \equiv \vec{\vartheta}_{j_\mathbb{R}} + \vec{\vartheta}_{j_\mathbb{I}} + \vec{\vartheta}_{jZ} \equiv \left(\vec{\vartheta}_j\right) \equiv \left(\vec{\vartheta}_{j_\mathbb{R}}, \vec{\vartheta}_{j_\mathbb{I}}, \vec{\vartheta}_{jZ}\right) \equiv \left(|\vec{\vartheta}_j|, \langle \vec{\vartheta}_j \rangle, [\vec{\vartheta}_j]\right), \tag{33}$$

such that

$$\begin{aligned} \vec{\vartheta}_{j_\mathbb{R}} &\equiv \vec{v}_{j_\mathbb{R}} - \vec{v}_{O_\mathbb{R}} \\ \vec{\vartheta}_{j_\mathbb{I}} &\equiv \vec{v}_{j_\mathbb{I}} - \vec{v}_{O_\mathbb{I}} \\ \vec{\vartheta}_{jZ} &\equiv \vec{v}_{jZ} - \vec{v}_{O_Z}, \end{aligned} \tag{34}$$

where from eq. (49) in [29] we establish

$$\begin{aligned} |\vec{\vartheta}_j| &\equiv \sqrt{\vec{\vartheta}^2_{j_\mathbb{R}} + \vec{\vartheta}^2_{j_\mathbb{I}} + \vec{\vartheta}^2_{jZ}} \\ \langle \vec{\vartheta}_j \rangle &\equiv \arctan\left(\frac{\vec{\vartheta}_{j_\mathbb{I}}}{\vec{\vartheta}_{j_\mathbb{R}}}\right) \\ [\vec{\vartheta}_j] &\equiv \arccos\left(\frac{\vec{\vartheta}_{jZ}}{|\vec{\vartheta}_j|}\right), \end{aligned} \tag{35}$$

which is clearly similar to the constraints of eqs. (26) and (29) that follow [29].

We note that the spherical time-dimension $T \subset Y$ in eq. (40) of [29] with amplitude-radius ϵ does apply to this scenario, but we must wait to establish T in Section 3.2 because the value of ϵ depends on the NGNBSSA's intermediate results. A 3D-PPS that exists in T is defined as a *time-effective 3D-PPS* (TE-3D-PPS); the 3D-PPM, 3D-NFFOPS, 3D-NAFOPS, 3D-VFOPS, and 3D-RVFOPS for a TE-3D-PPS are defined as the *time-effective 3D-PPM*(TE-3D-PPM), *time-effective 3D-NFFOPS* (TE-3D-NFFOPS), *time-effective 3D-NAFOPS* (TE-3D-NAFOPS), *time-effective 3D-VFOPS* (TE-3D-VFOPS), and *time-effective 3D-RVFOPS* (TE-3D-RVFOPS), respectively. Thus, at this point, we can encode the relevant chaotic dynamical system states in the Riemannian dual 4D space-time of [29] for the upcoming NGNBSSA in Section 3.2.

3 Algorithm

In this section, we explain *how* certain aspects of Newton's n PPM problem can be reduced to a two PPM problem in the holographic principle context; for this, the complete NGNBSSA is communicated via an example. The NGNBSSA's ultimate objective is to partition the n PPMs into two PPMs for a time-effective framework. To summarize, we arbitrarily select one PPM, namely the *Origin Position-Point-Mass* (O-PPM), and subsequently engage a series of *Time-Effective Spherical Normalization Adjustment* (TESNA) instructions to consolidate the residual $(n-1)$ PPMs to a single *Holographic Position-Point-Mass* (H-PPM), where the location and feature vectors of the $(n-1)$ PPMs are summed to produce net vectors for the H-PPM. The H-PPM represents the mass of the time-effective spherical surface T with amplitude-radius ϵ from [29, 30] for which the gravitational force and relative effects are preserved under the TESNAs. From there, we demonstrate that it is possible calculate the *net* time-effective quantities between the O-PPM and the H-PPM so we may exercise the effective potential, kinetic, and Lagrangian definitions in the quark confinement proof of [30].

In this systematic illustration, we choose to solve the $n = 3$ base case in dual 3D space-time due to its visualization simplicity—it is easier to draw Figures 1–6 on X and reduce three PPMs to two PPMs. But as we shall see, the guidelines of the NGNBSSA are kept generalized and can be directly applied to $(n > 3)$ PPMs. Moreover, the NGNBSSA is *almost identical* for both 3D and 4D space-time scenarios. Thus, in Section 3.1, we introduce and define the NGNBSSA with step-by-step depictions for dual 3D space-time. Then in Section 3.2, we explain precisely how to apply it to dual 4D space-time by simply "swapping out" the data structures and making a couple of slight algorithmic adjustments.

3.1 Complex algorithm for dual 3D space-time

The three 2D-PPM illustration for the NGNBSSA in dual 3D space-time is defined by the following sequence:

- **Routine 1:** Particle Initialization

  1. Randomly generate or experimentally identify $n = 3$ distinct 2D-PPSs on X to create the ordered 2D-PPS set P_X in the form of eq. (1) with the 2D Riemannian-coordinates of eq. (2); *we let these 2D-PPSs be*

  $$P_X \subset X = \{\vec{x}_A, \vec{x}_B, \vec{x}_C\}$$

  (for this example, we assert that $\vec{x}_B$ and $\vec{x}_C$ are different distances from $\vec{x}_A$ for illustration purposes, but certainly this is not a necessary requirement).

  2. Randomly assign or experimentally measure the three 2D-PPMs to create the ordered 2D-PPM set M_X in the form of eq. (3) that correspond to the established 2D-PPSs of P_X; *let*

  $$M_X = \{m_A, m_B, m_C\}$$

  be the ordered 2D-PPM set of three 2D-PPM elements that respectively correspond to P_X, such that $m_A, m_B, m_C > 0$.

  3. Randomly assign or experimentally measure the three 2D-VFOPSs to create the ordered 2D-VFOPS set V_X of eq. (4) in the form of eq. (5) that correspond to

the established 2D-PPSs of P_X; *let*

$$V_X = \{\vec{v}_A, \vec{v}_B, \vec{v}_C\}$$

be the ordered 2D-VFOPS set of three 2D-VFOPS elements that respectively correspond to P_X.

4. See Figure 1.

- **Routine 2:** Dual Space-Time Topology Initialization

1. Arbitrarily select a 2D-PPS from P_X; *let us choose* $\vec{x}_A \in P_X$.
2. Determine the closest 2D-PPS to the selected $\vec{x}_A$ using the 2D Euclidean distance from eq. (8); *we determine that* $\vec{x}_B \in P_X$ *is the closest to the selected* $\vec{x}_A$*, where the distance between them is* d_{AB}.
3. Draw the topological circle $T \subset X$ to represent the time zone from eq. (13) in [29], where the selected $\vec{x}_A$ is T's center, such that $\vec{x}_B$ lies precisely on T; *we construct the circle* $T \subset X$ *with center* $\vec{x}_A$*, where* T*'s amplitude-radius* ϵ *from eq. (15) in [29] is equal to the Euclidean distance* d_{AB} *between* $\vec{x}_A$ *and* $\vec{x}_B$*, so* $d_{AB} = \epsilon$ *for the geometrical line segment* $\overline{\vec{x}_A\vec{x}_B}$*, such that* $\vec{x}_B \in T$.
4. Label the spatial sub-surfaces that are simultaneously dual to T; T *topologically delineates the "micro space zone"* $X_- \subset X$ *and "macro space zone"* $X_+ \subset X$ *for the "space-time duality" in [29, 30].*
5. See Figure 2.

- **Routine 3:** Reference Frame, O-PPM, and OPS Assignment

1. Designate the selected $\vec{x}_A$ as the origin-point O of X to establish the reference frame; *we re-name* $\vec{x}_A$ *as* O *to thereby assign* $O = \vec{x}_A$ *as the point-of-reference, and additionally re-name the 2D-PPM* m_A *as the 2D-O-PPM of* X *to thereby assign* $m_O = m_A$.
2. Use eqs. (9–10) to assign 2D-NFFOPSs to the 2D-PPM that is the closest to m_O, namely m_B at $\vec{x}_B$, and all remaining 2D-PPMs in M_X (which is just m_C at $\vec{x}_C$); *for* O *and* $\vec{x}_B$*, the 2D-NFFOPS between the corresponding* m_O *and* m_B *is*

$$\vec{F}_B = \vec{F}_{B_{\mathbb{R}}} + \vec{F}_{B_{\mathbb{I}}} = (\vec{F}_B) = (|\vec{F}_B|, \langle\vec{F}_B\rangle) = (\vec{F}_{B_{\mathbb{R}}}, \vec{F}_{B_{\mathbb{I}}}),$$

such that

$$|\vec{F}_B| = G\frac{m_O m_B}{|\vec{x}_B|^2} = G\frac{m_O m_B}{|d_B|^2} = G\frac{m_O m_B}{\epsilon^2}$$
$$\langle\vec{F}_B\rangle = \langle\vec{x}_B\rangle,$$

and for O *and* $\vec{x}_C$*, the 2D-NFFOPS between the corresponding* m_O *and* m_C *is*

$$\vec{F}_C = \vec{F}_{C_{\mathbb{R}}} + \vec{F}_{C_{\mathbb{I}}} = (\vec{F}_C) = (|\vec{F}_C|, \langle\vec{F}_C\rangle) = (\vec{F}_{C_{\mathbb{R}}}, \vec{F}_{C_{\mathbb{I}}}),$$

such that

$$
\begin{aligned}
|\vec{F}_C| &= G\frac{m_O m_C}{|\vec{x}_C|^2} = G\frac{m_O m_B}{|d_C|^2} \\
\langle \vec{F}_C \rangle &= \langle \vec{x}_C \rangle.
\end{aligned}
$$

3. Use eqs. (12–13) to assign 2D-NAFOPSs to $m_B, m_C \in M_X$, with respect to m_O; *for O and $\vec{x}_B$, the 2D-NAFOPS between the corresponding m_O and m_B is*

$$
\vec{a}_B = \vec{a}_{B_\mathbb{R}} + \vec{a}_{B_\mathbb{I}} = (\vec{a}_B) = (|\vec{a}_B|, \langle \vec{a}_B \rangle) = (\vec{a}_{B_\mathbb{R}}, \vec{a}_{B_\mathbb{I}}),
$$

such that

$$
\begin{aligned}
|\vec{a}_B| &= \frac{|\vec{F}_B|}{m_B} \\
\langle \vec{a}_B \rangle &= \langle \vec{F}_B \rangle = \langle \vec{x}_B \rangle,
\end{aligned}
$$

and for O and $\vec{x}_C$, the 2D-NAFOPS between the corresponding m_O and m_C is

$$
\vec{a}_C = \vec{a}_{C_\mathbb{R}} + \vec{a}_{C_\mathbb{I}} = (\vec{a}_C) = (|\vec{a}_C|, \langle \vec{a}_C \rangle) = (\vec{a}_{C_\mathbb{R}}, \vec{a}_{C_\mathbb{I}}),
$$

such that

$$
\begin{aligned}
|\vec{a}_C| &= \frac{|\vec{F}_C|}{m_B} \\
\langle \vec{a}_C \rangle &= \langle \vec{F}_C \rangle = \langle \vec{x}_C \rangle.
\end{aligned}
$$

4. Relative to m_O with $\vec{v}_O$, use eqs. (15–17) to assign 2D-RVFOPSs to $m_B, m_C \in M_X$ with $\vec{v}_B, \vec{v}_C \in V_X$; *for O and $\vec{x}_B$, the 2D-RVFOPS for the corresponding $\vec{v}_O$ and $\vec{v}_B$ is*

$$
\vec{\vartheta}_B = \vec{\vartheta}_{B_\mathbb{R}} + \vec{\vartheta}_{B_\mathbb{I}} = (\vec{\vartheta}_B) = (|\vec{\vartheta}_B|, \langle \vec{\vartheta}_B \rangle) = (\vec{\vartheta}_{B_\mathbb{R}}, \vec{\vartheta}_{B_\mathbb{I}}),
$$

such that

$$
\begin{aligned}
\vec{\vartheta}_{B_\mathbb{R}} &= \vec{v}_{B_\mathbb{R}} - \vec{v}_{O_\mathbb{R}} = |\vec{\vartheta}_B| \cos\langle \vec{\vartheta}_B \rangle \\
\vec{\vartheta}_{B_\mathbb{I}} &= \vec{v}_{B_\mathbb{I}} - \vec{v}_{O_\mathbb{I}} = |\vec{\vartheta}_B| \sin\langle \vec{\vartheta}_B \rangle \\
|\vec{\vartheta}_B| &= \sqrt{\vec{\vartheta}^2_{B_\mathbb{R}} + \vec{\vartheta}^2_{B_\mathbb{I}}},
\end{aligned}
$$

and for O and $\vec{x}_C$, the 2D-RVFOPS for the corresponding $\vec{v}_O$ and $\vec{v}_C$ is

$$
\vec{\vartheta}_C = \vec{\vartheta}_{C_\mathbb{R}} + \vec{\vartheta}_{C_\mathbb{I}} = (\vec{\vartheta}_C) = (|\vec{\vartheta}_C|, \langle \vec{\vartheta}_C \rangle) = (\vec{\vartheta}_{C_\mathbb{R}}, \vec{\vartheta}_{C_\mathbb{I}}),
$$

such that

$$
\begin{aligned}
\vec{\vartheta}_{C_\mathbb{R}} &= \vec{v}_{C_\mathbb{R}} - \vec{v}_{O_\mathbb{R}} = |\vec{\vartheta}_C| \cos\langle \vec{\vartheta}_C \rangle \\
\vec{\vartheta}_{C_\mathbb{I}} &= \vec{v}_{C_\mathbb{I}} - \vec{v}_{O_\mathbb{I}} = |\vec{\vartheta}_C| \sin\langle \vec{\vartheta}_C \rangle \\
|\vec{\vartheta}_C| &= \sqrt{\vec{\vartheta}^2_{C_\mathbb{R}} + \vec{\vartheta}^2_{C_\mathbb{I}}}.
\end{aligned}
$$

5. See Figure 3.

- **Routine 4:** TESNA Application to Non-Temporal 2D-PPMs

1. Use X's built-in space-time duality of eq. (17) in [29] to map all the 2D-PPMs that are currently in X_+ to T to acquire the TE-2D-PPSs that share the uniform amplitude-radii ϵ (for spherical normalization), where these mappings are TESNAs that satisfy the the *TESNA Constraints* (TESNAC)
   - Phase-TESNAC: the 2D-PPMs in X_+ and their corresponding TE-2D-PPMs in T must have equivalent 2D-PPS-phases, TE-2D-PPS-phases, 2D-NFFOPS-phases, TE-2D-NFFOPS-phases, 2D-NAFOPS-phases, and TE-2D-NAFOPS-phases (to preserve the directional effect), and
   - NFFOPS-amplitude-TESNAC: the 2D-PPMs in X_+ and the corresponding TE-2D-PPMs in T must have equivalent 2D-NFFOPS-amplitudes and TE-2D-NFFOPS-amplitudes (to preserve the force effect);

   for the 2D-PPM m_C at the 2D-PPS $\vec{x}_C \in X_+$, we identify and create the corresponding TE-2D-PPM m_{C^*} at the TE-2D-PPS $\vec{x}_{C^*} \in T$, with the 2D-PPS TESNA

$$\vec{x}_C \to \vec{x}_{C^*}, \tag{36}$$

   and select/calculate the corresponding TE-2D-PPM solution m_{C^*}, such that $m_{C^*} \neq m_C$, which satisfies the Phase-TESNAC

$$\begin{aligned} \langle \vec{x}_{C^*} \rangle &= \langle \vec{x}_C \rangle = \langle \vec{F}_{C^*} \rangle = \langle \vec{F}_C \rangle = \langle \vec{a}_{C^*} \rangle = \langle \vec{a}_C \rangle \\ |\vec{x}_{C^*}| &\neq |\vec{x}_C| \Rightarrow \vec{x}_{C^*} \neq \vec{x}_C, \end{aligned} \tag{37}$$

   and also satisfies the 2D-NFFOPS-amplitude-TESNAC

$$\begin{aligned} |\vec{F}_{C^*}| &= |\vec{F}_C| = G\tfrac{m_O m_{C^*}}{d_{C^*}^2} = G\tfrac{m_O m_C}{d_C^2} = m_C|\vec{a}_C| = m_{C^*}|\vec{a}_{C^*}| \\ m_{C^*} &\neq m_C, \quad d_{C^*} \neq d_C, \quad d_{C^*} = \epsilon, \quad d_C \neq \epsilon \\ (|\vec{F}_{C^*}| &= |\vec{F}_C|) \wedge (d_{C^*} \neq d_C) \Rightarrow (m_{C^*} \neq m_C). \end{aligned} \tag{38}$$

2. See Figure 4.

- **Routine 5:** TE-2D-PPM Consolidation for Net 2D-PPM (or Net TE-2D-PPM) Identification

1. For all TE-2D-PPMs in T, sum the corresponding TE-2D-PPSs to calculate the *net 2D-PPS* for the *net 2D-PPM*; *for the TE-2D-PPMs m_B and m_{C^*} in T, we sum the corresponding TE-2D-PPSs $\{\vec{x}_B, \vec{x}_{C^*}\} \in T$ to determine the net 2D-PPS*

$$\vec{x}_D = \vec{x}_{net} = \vec{x}_B + \vec{x}_{C^*} \tag{39}$$

   for the net 2D-PPM m_D.

2. For all TE-2D-PPMs in T, sum the corresponding TE-2D-NFFOPSs to calculate the *net 2D-NFFOPS* for the *net 2D-PPM*; *for the TE-2D-PPMs* m_B *and* m_{C^*} *in* T*, we sum the corresponding 2D-NFFOPSs* $\vec{F}_B$ *and* $\vec{F}_{C^*}$ *to determine the net 2D-NFFOPS*
$$\vec{F}_D = \vec{F}_{net} = \vec{F}_B + \vec{F}_{C^*}, \tag{40}$$
such that the net 2D-NFFOPS-amplitude is
$$|\vec{F}_D| = |\vec{F}_{net}| = G\frac{m_O m_D}{|\vec{x}_D|^2} = G\frac{m_O m_D}{d_D^2} = G\frac{m_O m_{net}}{d_{net}^2} \tag{41}$$
and the corresponding net 2D-NFFOPS-phase is
$$\langle\vec{F}_D\rangle = \langle\vec{F}_{net}\rangle = \langle\vec{x}_D\rangle = \langle\vec{x}_{net}\rangle \tag{42}$$
for the net 2D-PPM $m_D = m_{net}$.

3. For the net 2D-PPM m_D, use the results of eqs. (39–42) to calculate the *net 2D-NAFOPS*; *for the net 2D-PPM* m_D*, the net 2D-NAFOPS* $\vec{a}_D = \vec{a}_{net}$ *has the net 2D-NAFOPS-amplitude*
$$|\vec{a}_D| = |\vec{a}_{net}| = \frac{|\vec{F}_D|}{m_D} = \frac{|\vec{F}_{net}|}{m_{net}} \tag{43}$$
and the net 2D-NAFOPS-phase
$$\langle\vec{a}_D\rangle = \langle\vec{a}_{net}\rangle = \langle\vec{F}_D\rangle = \langle\vec{F}_{net}\rangle = \langle\vec{x}_D\rangle = \langle\vec{x}_{net}\rangle, \tag{44}$$
so now there are just two 2D-PPMs to deal with, namely m_O *and* m_D*!*

4. Determine if the net 2D-PPM m_D is a net TE-2D-PPM on T; *we observe that* $\vec{x}_D \notin T$ *and* $\vec{x}_D \neq O$*, but rather* $\vec{x}_D \in X_+$*, so we proceed to Routine 6 because* m_D *is not a net TE-2D-PPM and we require a net TE-2D-PPM on* T *to label it the H-PPM and finish.*

5. See Figure 5.

- **Routine 6:** H-PPM Identification

1. Similarly to Routine 4, we employ X's space-time duality to TESNA map the net 2D-PPM m_D to its corresponding *net TE-2D-PPM* m_{D^*} on T in accordance to the TESNACs so m_{D^*} with $\vec{x}_{D^*} \in T$ becomes the H-PPM; *for the net 2D-PPS* $\vec{x}_D \in X_+$ *we identify the corresponding net TE-2D-PPS* $\vec{x}_{D^*} \in T$ *with the TESNA*
$$\vec{x}_D \to \vec{x}_{D^*} \tag{45}$$
and select/calculate the corresponding net TE-2D-PPM solution m_{D^*}*, such that* $m_{D^*} \neq m_D$*, which satisfies the Phase-TESNAC*
$$\begin{aligned} \langle\vec{x}_{D^*}\rangle &= \langle\vec{x}_D\rangle = \langle\vec{F}_{D^*}\rangle = \langle\vec{F}_D\rangle = \langle\vec{a}_{D^*}\rangle = \langle\vec{a}_D\rangle \\ |\vec{x}_{D^*}| &\neq |\vec{x}_D| \Rightarrow \vec{x}_{D^*} \neq \vec{x}_D, \end{aligned} \tag{46}$$

and also satisfies the 2D-NFFOPS-amplitude-TESNAC

$$
\begin{aligned}
|\vec{F}_{D^*}| &= |\vec{F}_D| = G\tfrac{m_O m_{D^*}}{d_{D^*}^2} = G\tfrac{m_O m_D}{d_D^2} = m_D|\vec{a}_D| = m_{D^*}|\vec{a}_{D^*}| \\
m_{D^*} &\neq m_D, \quad d_{D^*} \neq d_D, \quad d_{D^*} = \epsilon, \quad d_D \neq \epsilon \qquad (47) \\
(|\vec{F}_{D^*}| &= |\vec{F}_D|) \wedge (d_{D^*} \neq d_D) \Rightarrow (m_{D^*} \neq m_D),
\end{aligned}
$$

so finally we know all of the net time-effective quantities that are required to encode the chaotic system state because m_{D^*} is now the net TE-2D-PPM and H-PPM for T!

2. See Figure 6.

Thus, from eq. (50) in [30], the NGNBSSA's time-effective Lagrangian for m_O and m_{D^*} is defined as

$$\mathcal{L}[m_O, \vec{x}_{D^*}, m_{D^*}, \vec{\vartheta}_{D^*}] \equiv E_K[m_{D^*}, \vec{\vartheta}_{D^*}] - E_P[m_O, \vec{x}_{D^*}] \qquad (48)$$

using our generalized coordinates, where E_K and E_P are the time-effective kinetic and time-effective potential, respectively, for the H-PPM m_{D^*} relative to the O-PPM m_O. Using eq. (51) in [30] we define the time-effective potential E_P between m_O and m_{D^*} as

$$E_P[m_O, \vec{x}_{D^*}] \equiv \frac{\sqrt{1 - 2\left(\frac{m_O}{|\vec{x}_{D^*}|}\right)}}{|\vec{x}_{D^*}|} \equiv \frac{\sqrt{1 - 2\left(\frac{m_O}{\epsilon}\right)}}{\epsilon}, \qquad (49)$$

and subsequently employ eq. (52) in [30] to define the corresponding time-effective kinetic E_K as

$$E_K[m_{D^*}, \vec{\vartheta}_{D^*}] \equiv \frac{1}{2} m_{D^*} |\vartheta_{D^*}|^2 \equiv \frac{1}{2}\left(\frac{|\vec{F}_{D^*}|}{|a_{D^*}|}\right)|\vartheta_{D^*}|^2, \qquad (50)$$

where ϑ_{D^*} is the *time-effective net 2D-RVFOPS* of m_{D^*} at $\vec{x}_{D^*}$ relative to m_O at O in the dual 3D space-time of X.

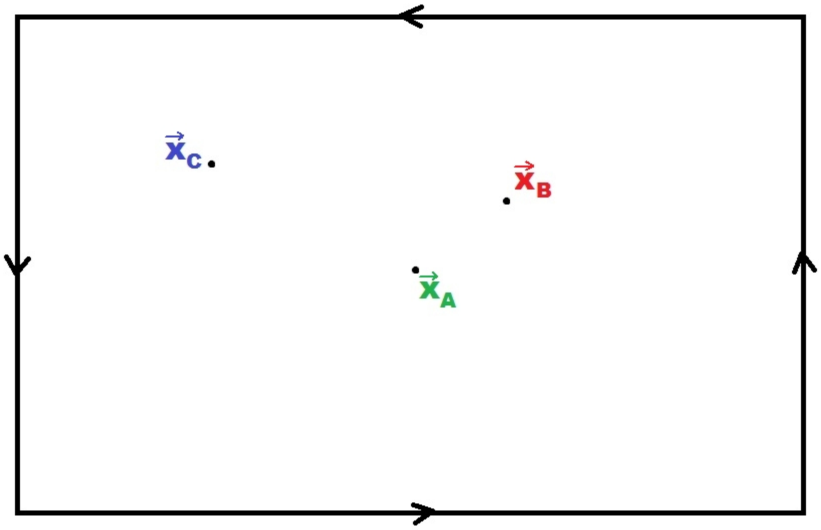

Fig. 1: The Routine 1 depiction of the $n = 3$ NGNBSSA. The three 2D-PPSs $\{\vec{x}_A, \vec{x}_B, \vec{x}_C\} = P_X \subset X$ correspond to the ordered 3-body set $\{m_A, m_B, m_C\} = M_X$.

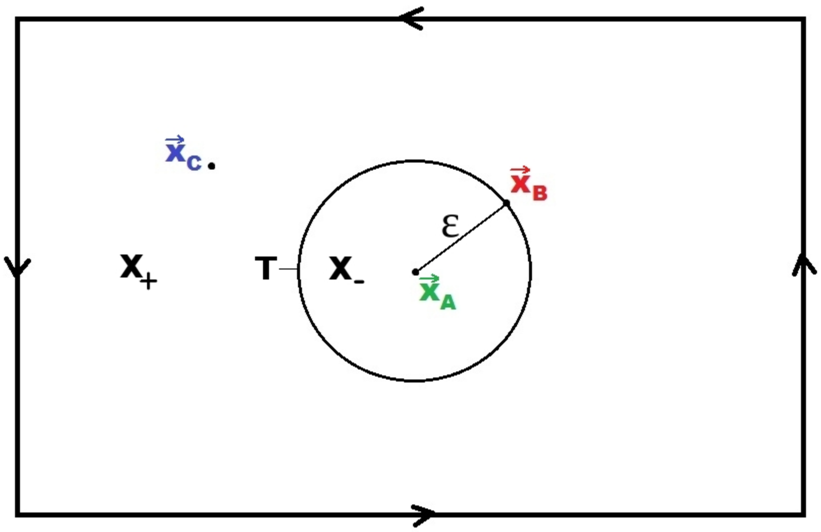

Fig. 2: The Routine 2 depiction of the $n = 3$ NGNBSSA. The 2D-PPS $\vec{x}_A$ is the center of the topological circle and time zone $T \subset X$, which is isometrically embedded on X, where $\vec{x}_B \in T$.

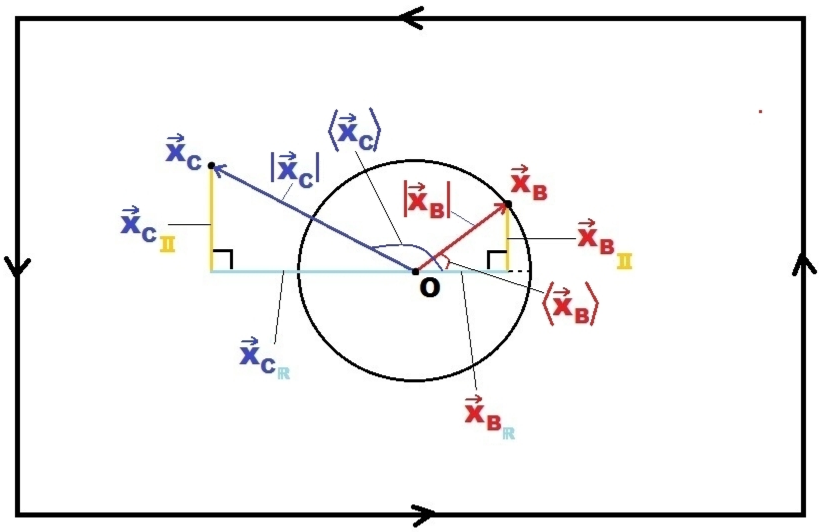

Fig. 3: The Routine 3 depiction of the $n = 3$ NGNBSSA. The 2D-PPS $O = \vec{x}_A$ becomes X's origin-point for the reference frame. Using Newton's laws, we assign 2D-NFFOPSs and 2D-NAFOPSs to the 2D-PPMs m_B and m_C located at the 2D-PPSs $\vec{x}_B$ and $\vec{x}_C$, respectively, such that $|\vec{x}_B| = \epsilon$ and $|\vec{x}_C| \neq \epsilon$, respectively.

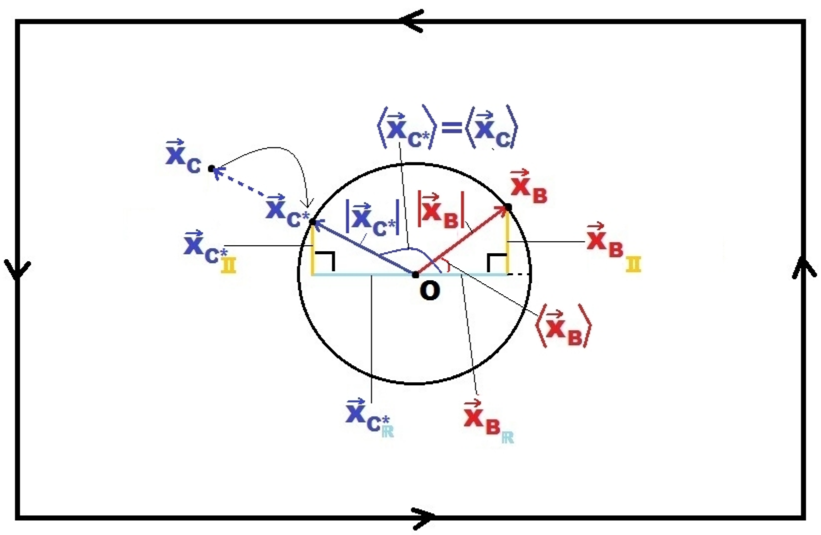

Fig. 4: The Routine 4 depiction of the $n = 3$ NGNBSSA. The objective is to TESNA map all non-temporal 2D-PPSs (except for the origin-point) to T so one 2D-PPM, namely the O-PPM m_O, is at O, while the residual $(n-1)$ 2D-PPMs are mapped to T to prepare for construction of the upcoming net TE-2D-PPM and H-PPM. The procedure adheres to the Phase-TESNAC and the 2D-NFFOPS-amplitude-TESNAC that enable us simplify the problem state with TESNAs. Here, we have $\vec{x}_B \in T$, so the 2D-PPM m_B already lies precisely on T. But $\vec{x}_C \in X_+$, so $\vec{x}_C \notin T$ is a non-temporal 2D-PPS, thus we must use X's built-in "space-time duality" to use the TESNA $\vec{x}_C \to \vec{x}_{C^*}$ to create the corresponding TE-2D-PPM solution m_{C^*} for T because we need some $\vec{x}_{C^*} \in T$.

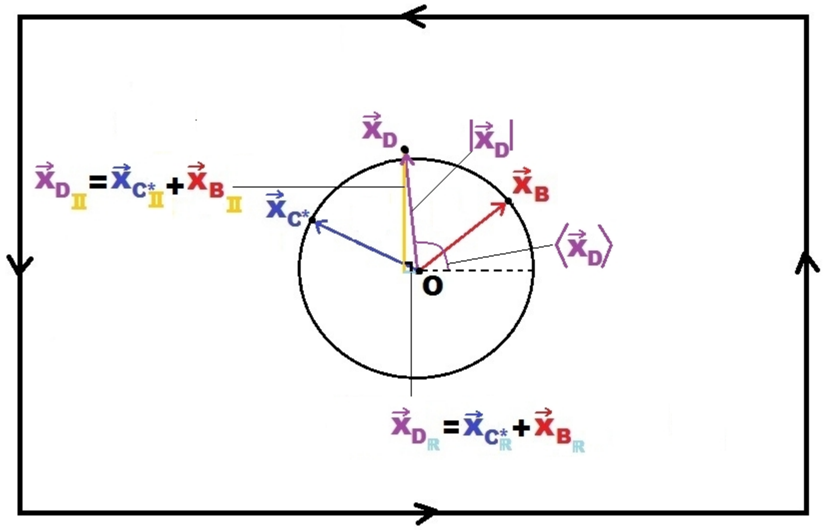

Fig. 5: The Routine 5 depiction of the $n = 3$ NGNBSSA. The *net 2D-NFFOPS* $\vec{F}_D$ is the 2D-NFFOPS sum of $\vec{F}_B$ and $\vec{F}_{C^*}$ for the resulting gravitational force field that corresponds to a *net 2D-PPS* $\vec{x}_D$ with a *net 2D-PPM* m_D. This consolidates the residual $(n-1)$ 2D-PPMs to m_D to establish a time-effective 2-body system composed of m_O and m_D; now there are just 2-bodies to deal with!

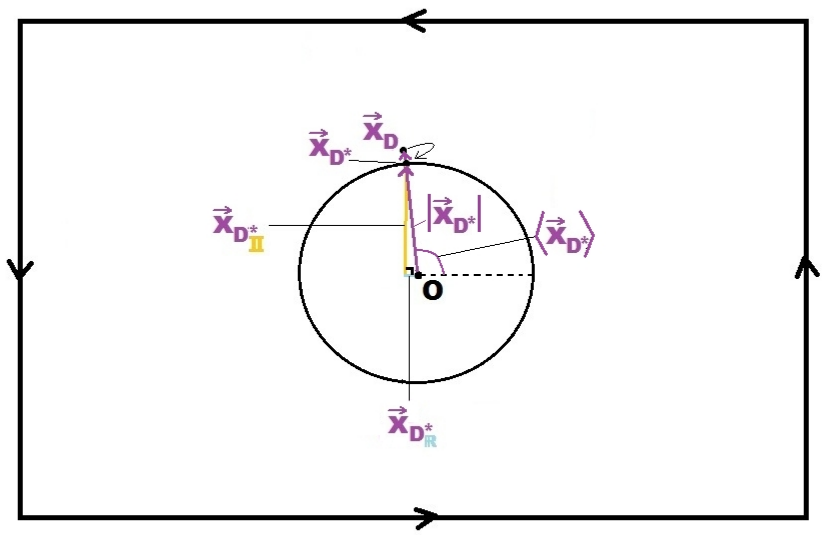

Fig. 6: The Routine 6 depiction of the $n = 3$ NGNBSSA. So $\vec{x}_D \notin T$, thus for $\vec{x}_D \in X_+$ we identify the corresponding $\vec{x}_{D^*} \in T$ via the TESNA $\vec{x}_D \to \vec{x}_{D^*}$ to calculate the single *net TE-2D-PPM* m_{D^*}, namely the H-PPM. Now we've finally delivered a gravitationally normalized time-effective 2-body system of m_O and m_{D^*}!

3.2 Triplex algorithm for dual 4D space-time

So how do we apply our NGNBSSA to dual 4D space-time? Well first, we recall that in Section 2.2 we've already provided a working triplex framework for encoding locations and features in the 4D space-time topology. Hence, our initial step is to revisit the NGNBSSA of Section 3.1 and simply swap the complex data structures in Section 2.1 with their triplex counterparts in Section 2.2. Moreover, we also recall that the NGNBSSA is almost identical for both 3D and 4D space-time scenarios, $\forall n > 2$, but there are a couple of slight modifications that we need to make:

- **In Routine 1**

  1. Replace the 2D-PPSS X with the 3D-PPSS Y.
  2. Replace the ordered 2D-PPS set P_X of eqs. (1–2) with the ordered 3D-PPS set P_Y of eqs. (18–19).
  3. Replace the ordered 2D-PPM set M_X of eq. (3) with the ordered 3D-PPM set M_Y of eq. (20).
  4. Replace the ordered 2D-VFOPS set V_X of eqs. (4–5) with the ordered 3D-VFOPS set V_Y of eqs. (21–22).

- **In Routine 2**

  1. Use the 3D Euclidean distance of eq. (25) instead of the 2D Euclidean distance of eq. (8).
  2. Define T with the triplex form of eq. (40) in [29] rather than the complex form of eq. (15) in [30].

- **In Routine 3**

  1. Replace the 2D-NFFOPS notation of eq. (9) with the 3D-NFFOPS notation of eq. (26) and add the pertinent 3D-NFFOPS-inclination equivalences.
  2. Replace the 2D-NAFOPS notation of eq. (12) with the 3D-NAFOPS notation of eq. (29) and add the pertinent 3D-NAFOPS-inclination equivalences.
  3. Replace the 2D-RVFOPS notation of eq. (15) with the 3D-RVFOPS notation of eq. (33).

- **In Routine 4**

  1. Create, define, and apply the Inclination-TESNAC

  $$[\vec{y}_{C^*}] = [\vec{y}_C] = [\vec{F}_{C^*}] = [\vec{F}_C] = [\vec{a}_{C^*}] = [\vec{a}_C] \tag{51}$$

  to extend the TESNAs to an additional degree of freedom.

- **In Routine 5**

1. Replace T's TE-2D-PPM construction with a TE-3D-PPM construction.

- **In Routine 6**

  1. Apply the Inclination-TESNAC of Routine 4 to finalize construction of T's TE-3D-PPM and H-PPM.

Thus, we've listed the requisite modifications to apply the NGNBSSA to the dual 4D space-time.

At this point, complex time-effective Lagrangian definition of eq. (48) is re-written in the triplex form

$$\mathcal{L}[m_O, \vec{y}_{D^*}, m_{D^*}, \vec{\vartheta}_{D^*}] \equiv E_K[m_{D^*}, \vec{\vartheta}_{D^*}] - E_P[m_O, \vec{y}_{D^*}], \tag{52}$$

so eq. (49) becomes

$$E_P[m_O, \vec{y}_{D^*}] \equiv \frac{\sqrt{1 - 2\left(\frac{m_O}{|\vec{y}_{D^*}|}\right)}}{|\vec{y}_{D^*}|} \equiv \frac{\sqrt{1 - 2\left(\frac{m_O}{\epsilon}\right)}}{\epsilon}, \tag{53}$$

and eq. (50) becomes

$$E_K[m_{D^*}, \vec{\vartheta}_{D^*}] \equiv \frac{1}{2} m_{D^*} |\vartheta_{D^*}|^2 \equiv \frac{1}{2}\left(\frac{|\vec{F}_{D^*}|}{|a_{D^*}|}\right)|\vartheta_{D^*}|^2 \tag{54}$$

in the dual 4D space-time of Y.

4 Conclusion and discussion

In this preliminary paper, we introduced, defined, and constructed a framework that is designed to simplify certain aspects of Newton's gravitational n-body problem. We started by outlining the importance of further comprehending the chaos inherent to this natural problem, which applies to multiple and diverse realms within the disciplines of science, mathematics, computation, and engineering. Subsequently, we assembled the dual space-time topology, generalized coordinate system, and order parameter data structures to implement our NGNBSSA. During this pursuit, we demonstrated that our framework provides an abstract, powerful, and flexible state space encoding methodology for chaotic gravitational systems with creative applications to mathematics and physics. Moreover, we found that the NGNBSSA and its structural framework encompass a relatively simplistic formulation which enables us to represent variable degrees of complexity for this mode of analysis.

For the future, we suggest that this model should be extended to include additional aspects of classical, quantum, and relativistic mechanics for physics, chaos, and fractal geometry. It would be intriguing to implement our NGNBSSA on a super-computing cluster so one can conduct parallel simulations to further refine the direct practicality of these ideas. Also, it may be beneficial to match the predictions of this theory with real-time astronomical data and conduct high-energy physics experiments to prove (or disprove) pertinence to hadronic mechanics.

In our opinion, the NGNBSSA is a powerful systematic process with an *enormous* potential for direct application to modern physics—theoretical *and* experimental. So although this model is still under development, we suspect that through further investigation, scrutiny, refinement, collaboration, and hard work, these ideas may reveal additional key facets in mathematics, computation, engineering, and science.

5 Acknowledgment

We wish to thank an anonymous referee for the useful comments and constructive criticism that authorized us to upgrade the content of this paper.

References

[1] B. M. Gessen and J. Herivel. *The background to Newton's Principia: a study of Newton's dynamical researches in the years 1664-84*. Clarendon Press, 1965.

[2] I. Newton. *Principia, vol. I: the motion of bodies*. University of California Press, 1966.

[3] K. Huang and C. N. Yang. Quantum-mechanical many-body problem with hard-sphere interaction. *Physical review*, 105(3):767, 1957.

[4] T. D. Lee and C. N. Yang. Many-body problem in quantum mechanics and quantum statistical mechanics. *Physical Review*, 105(3):1119, 1957.

[5] F. E. Udwadia and R. E. Kalaba. *Analytical dynamics: a new approach*. Cambridge University Press, 2007.

[6] N. H. March, W. H. Young, and S. Sampanthar. *The many-body problem in quantum mechanics*. Courier Dover Publications, 1967.

[7] A. D. Bruno. *The restricted 3-body problem: plane periodic orbits*, volume 17. de Gruyter, 1994.

[8] S. H. Kellert. *In the wake of chaos: Unpredictable order in dynamical systems*. University of Chicago Press, 1993.

[9] E. N. Lorenz. *The essence of chaos*. Routledge, 1995.

[10] G. W. Flake. *The computational beauty of nature: Computer explorations of fractals, chaos, complex systems and adaption*. The MIT Press, 1998.

[11] J. Briggs. *Fractals: The patterns of chaos: A new aesthetic of art, science, and nature*. Touchstone Books, 1992.

[12] A. A. Tsonis and J. B. Elsner. Chaos, strange attractors, and weather. *Bulletin of the American Meteorological Society*, 70:14–23, 1989.

[13] J. Huisman and F. J. Weissing. Biodiversity of plankton by species oscillations and chaos. *Nature*, 402(6760):407–410, 1999.

[14] P. Philippe. Chaos, population biology, and epidemiology: some research implications. *Human Biology*, 65(4):525, 1993.

[15] P. Duesberg. Chromosomal chaos and cancer. *Scientific American Magazine*, 296(5):52–59, 2007.

[16] G. A. Calin, C. Vasilescu, M. Negrini, and G. Barbanti-Brodano. Genetic chaos and antichaos in human cancers. *Medical hypotheses*, 60(2):258–262, 2003.

[17] L. Bos and et al. *Plant viruses, unique and intriguing pathogens: a textbook of plant virology.* Backhuys Publishers, 1999.

[18] H. J. Xu and L. Knopoff. Periodicity and chaos in a one-dimensional dynamical model of earthquakes. *Physical Review E*, 50(5):3577, 1994.

[19] C. H. Scholz. Earthquakes as chaos. *Nature*, 348(6298):197–198, 1990.

[20] S. L. Harris. *Agents of chaos: earthquakes, volcanoes, and other natural disasters.* Mountain Press Publishing Company, 1990.

[21] B. LeBaron and B. LeBaron. Chaos and nonlinear forecastability in economics and finance. *Philosophical Transactions of the Royal Society of London. Series A: Physical and Engineering Sciences*, 348(1688):397–404, 1994.

[22] H. O. Peitgen, H. Jürgens, and D. Saupe. *Chaos and fractals: new frontiers of science.* Springer, 2004.

[23] B. B. Mandelbrot. *The fractal geometry of nature*. Times Books, 1982.

[24] G. B. West, J. H. Brown, and B. J. Enquist. A general model for the origin of allometric scaling laws in biology. *Science*, 276(5309):122–126, 1997.

[25] G. B. West, J. H. Brown, and B. J. Enquist. The fourth dimension of life: fractal geometry and allometric scaling of organisms. *Science*, 284(5420):1677–1679, 1999.

[26] R. Wu, C. X. Ma, R. C. Littell, and G. Casella. A statistical model for the genetic origin of allometric scaling laws in biology. *Journal of theoretical biology*, 219(1):121–135, 2002.

[27] G. B. West and J. H. Brown. The origin of allometric scaling laws in biology from genomes to ecosystems: towards a quantitative unifying theory of biological structure and organization. *Journal of Experimental Biology*, 208(9):1575–1592, 2005.

[28] L. Demetrius. The origin of allometric scaling laws in biology. *Journal of theoretical biology*, 243(4):455–467, 2006.

[29] N. O. Schmidt. A complex and triplex framework for encoding the riemannian dual space-time topology equipped with order parameter fields. *The Hadronic Journal*, 35(6):671, 2012.

[30] A. E. Inopin and N. O. Schmidt. Proof of quark confinement and baryon-antibaryon duality: I: Gauge symmetry breaking in dual 4D fractional quantum Hall superfluidic space-time. *The Hadronic Journal*, 35(5):469, 2012.